

Influence of Tacticity on the α Retardation Mode in Amorphous Poly(methyl methacrylate)

S. Doulut, P. Demont,* and C. Lacabanne

UMR CIRIMAT, Laboratoire de Physique des Polymères, Université Paul Sabatier, 31062 Toulouse, France

Received February 19, 1999; Revised Manuscript Received January 18, 2000

ABSTRACT: Thermally stimulated creep recovery (TSCR) experiments have been used to study the influence of tacticity on the α retardation process in amorphous poly(methyl methacrylate) (PMMA). The α retardation process associated with the glass transition is strongly dependent on tacticity. The high-sensitivity TSCR–fractional loading (FL) method was used to extract the distributions of activation enthalpies ΔH and entropies ΔS of the α mechanical relaxation. ΔH increases with temperature and is maximum at the glass transition temperature T_g . The maximum value and the full width at half-height of the activation enthalpy distribution are tacticity-dependent. Comparing experimental activation enthalpies with Starkweather's zero entropy prediction shows that the low-temperature tail of the α retardation process extends to 30 °C independent of tacticity. This result is attributed to the presence of isotriad sequences enhancing molecular mobility in this temperature range.

Introduction

The mechanical,¹ dielectric,² and thermal³ properties of poly(methyl methacrylate) (PMMA) are strongly dependent on the tacticity, i.e., the molecular configuration of the polymer chain. The glass transition temperature T_g is highly dependent on syndio-triad content and varies from 50 to 140 °C between isotactic and syndiotactic samples, respectively. There is actually no well-defined model to describe this behavior. Well-characterized PMMA samples of different tacticity have been investigated by Sauer and Kim using thermally stimulated depolarization current (TSDC).⁴ They characterized the broadness of the α relaxation in PMMA in terms of the magnitude of the values of activation enthalpy.⁴ To complete this dielectric characterization, we used thermally stimulated creep recovery (TSCR) as a very low equivalent frequency mechanical technique (5×10^{-3} Hz). The viscoelastic behavior study of PMMA in the T_g region is carried out using composite samples of multifilamented quartz braid and PMMA.

The advantage of TSCR is the experimental ability to resolve overlapping contributions to the α mechanical relaxation by using the fractional loading (FL) method.^{5–10} The FL-TSCR procedure allows the experimental deconvolution of a complex mechanical relaxation process into elementary relaxation processes. From the shape and temperature position of the isolated TSCR elementary peaks the corresponding kinetics parameters, i.e., activation enthalpy and entropy, are determined. The analysis of the temperature dependence of the activation enthalpy is carried out in the framework of the Starkweather's prediction of zero activation entropy.^{5,6}

Experimental Section

1. Materials. The narrow-distribution PMMA samples used in this study were obtained from Polymer Expert, ENSCPB, Bordeaux, France, by living anionic polymerization. The molecular weight M_w and the polydispersity index I_p were

determined by size exclusion chromatography (SEC). Table 1 shows several characterization data of the PMMA samples.

The tacticity of the samples was measured by means of ¹H NMR spectra obtained on a Bruker spectrometer. The amounts of syndio-, hetero-, and iso-triads were determined by measuring the relative areas of the different peaks observed at 0.85, 1.02, and 1.21 ppm, respectively. Samples are abbreviated in the text with reference to the syndio-triad percentage, i.e., S-36, S-63, and S-90, and to the iso-triad percentage as I-93.

The glass transition temperature T_g is determined using a Perkin-Elmer differential scanning calorimeter (DSC-7). The results are reported in Table 2 where T_g is defined as the midpoint of the heat capacity step ΔC_p at the glass transition. The as-received I-93 sample shows an endothermic peak at 130 °C associated with the melting process.¹⁴ To obtain amorphous PMMA I-93, the sample is annealed at 160 °C for 15 min and then quenched down to the TSCR loading temperature at a cooling rate of 40 °C min⁻¹.

2. Sample Preparation. TSCR experiments on low molecular weight samples throughout and above the glass transition are more easier when supported samples are used. To avoid irreversible flow in TSCR experiments at high temperatures ($T > T_g$), the as-received samples are deposited on a support. This support is an inert multifilamented quartz fibers braid in agreement with the Gillham's method.¹⁵ This material is chosen as substrate because it displays no mechanical retardation peaks and losses in the temperature range involved in this study. The dimensional stability of the sample is provided by the supporting substrate. The preparation sequence of TSCR samples is as follows: (i) A PMMA–THF solution with a concentration of 10 wt % is prepared. The sample S-36 is solubilized in chloroform. (ii) The solution is then poured out into a beaker, and the braid is dipped into the solution for 10 min to well impregnate all the quartz fibers. (iii) The solvent is evaporated by heating to 200 °C at a rate of 2 °C min⁻¹ under a helium atmosphere. This proceeding is repeated in situ after drying and degassing samples under high vacuum until no traces of solvent are observed by DSC and thermogravimetry analysis (TGA).

A comparison between thermomechanical spectra of the impregnated braid and the bulk sample is carried out to check that no artifacts occur in the TSCR response of the PMMA–quartz braid composite sample.¹⁶

3. Thermally Stimulated Creep Recovery Spectrometry. a. TSCR Complex Spectra. The TSCR principle and the torsion pendulum were extensively described else-

* Corresponding author. Tel 33 5 61 55 65 38; Telefax 33 5 61 55 62 21; e-mail demont@cict.fr.

Table 1. PMMA Samples Characterization

PMMA	M_n (g mol ⁻¹)	M_w (g mol ⁻¹)	I_p	syndio-triads %	iso-triads %	hetero-triads %
I-93	8 300	10 000	1.20	4	93	3
S-36	10 000 ^a	10 000 ^a	1	36	44	20
S-66	11 600	14 800	1.27	66	2	32
S-90	12 500	13 600	1.09	90	1	9

^a Molecular weight expected from synthesis conditions.

Table 2. Thermomechanical Properties of PMMA Samples

PMMA	T_g (±2 °C)	T_α (±2 °C)	ΔT_{DSC} (±4 °C)	ΔT_{TSCR} (±4 °C)
I-93	59	62	9	9
S-36	99	105	24	29
S-66	123	127	15	14
S-90	127	130	14	14

where,^{5–11,16} In a TSCR experiment, the sample, placed into the torsion pendulum, is submitted to a static shear stress σ at a given temperature T_o for 2 min. The sample, kept under stress, is quenched down to T_0 ($T_0 \ll T_o$) in order to freeze the induced strain. Then the stress is removed at T_0 and the recovery of the frozen-in strain γ measured during heating at 7 °C min⁻¹ to a final temperature T_f ($> T_o$). The rate of release of the frozen-in strain $\dot{\gamma}$ is recorded versus temperature and represents the TSCR complex spectrum.

b. Resolution of TSCR Complex Spectra by the Fractional Loading (FL) Method. Retardation spectra obtained by the TSCR experimental procedure are indicative of the nonisothermal creep recovery of the sample on a broad temperature range (generally more than 50 °C). This viscoelastic behavior can be described by a discrete distribution of retardation times.

The fractional loading (FL) method was applied to resolve the experimentally complex TSCR spectrum in elementary spectra well described by a simple rheological model.^{5–11,16} Fractional loading experiments are performed as follows: the stress σ is applied only in a narrow temperature window $T_o - T_{or} = \Delta T_o$, where T_{or} is the stress release temperature and $\Delta T_o = 3$ or 5 °C. The sample is then quenched down to T_0 , and the viscoelastic strain is frozen in. A linear heating scan at a rate of 7 °C min⁻¹ is then performed to record the decay of the frozen-in strain.

By varying T_s over the probed whole temperature range, a series of TSCR elementary peaks are obtained. Each fractional loading response is investigated using an analysis of FL-TSCR experiments proposed by Bucci, Fieschi, and Guidi (BFG plot).¹⁷ Here, each elementary recovery process can be characterized by a single retardation time τ , which is then determined by

$$\tau(T) = \left| \frac{\gamma(T)}{\dot{\gamma}(T)} \right| \quad (1)$$

where γ and $\dot{\gamma}$ are the strain and the rate of strain of the retardation process, respectively. When $\tau(T)$ obeys an Arrhenius law, the activation enthalpy ΔH and the preexponential factor τ_0 are obtained from

$$\tau(T) = \tau_0 \exp\left(\frac{\Delta H}{RT}\right) \quad (2)$$

where R is the gas constant. The activation entropy ΔS can also be derived from the Eyring¹⁸ equation:

$$\Delta S = R \ln\left(\frac{h}{k_B T \tau_0}\right) \quad (3)$$

where h and k_B are the Planck and Boltzmann constants, respectively. TSCR-FL experiments are performed in order

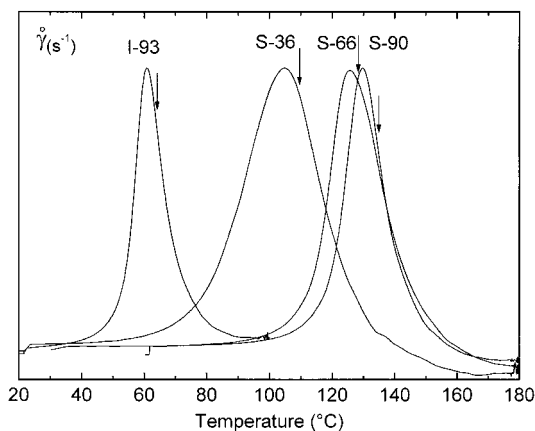


Figure 1. Complex TSCR spectra of I-93, S-36, S-66, and S-90 PMMA. The respective loading temperatures are symbolized by arrows.

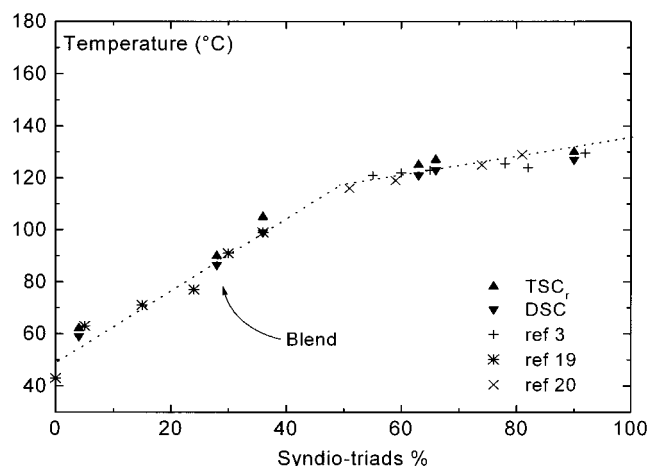


Figure 2. Glass transition temperature T_g and TSCR α peak maximum temperature as a function of syndio-triads percentage.

to study the detail of a retardation process (distribution of enthalpy and/or entropy).

Results

1. TSCR Complex Spectra. The TSCR complex spectra are shown in Figure 1 for PMMA samples of different tacticity. The spectra display a well-defined peak at T_α associated with the α relaxation or “dynamic” glass transition. The loading temperatures T_o are indicated by arrows. The main peak in the rate of release of the frozen-in strain occurs at temperature only depending on sample tacticity. The values of the TSCR peak temperature T_α are comparable to the DSC T_g values (see Table 2) and data available in the literature^{3,19,20} as reported in Figure 2 in terms of syndio-triads content. Agreement with literature data is good, and T_g and T_α increase with syndio-triads content. Unlike some literature assumptions,² T_g is not a linear function of syndio-triad content over the whole syndio-triad range. Nevertheless, two monotonic temperature behaviors are observed here and there of 50% of syndio-triads. The T_g values of 135 °C for a syndiotactic sample and 50 °C for an isotactic sample, both obtained from the extrapolation of the two temperature linear dependencies, are in agreement with literature data for pure tacticity samples.^{19,20}

2. Study of the “Fine Structure” of the TSCR Complex α Peak. Each sample was submitted to a

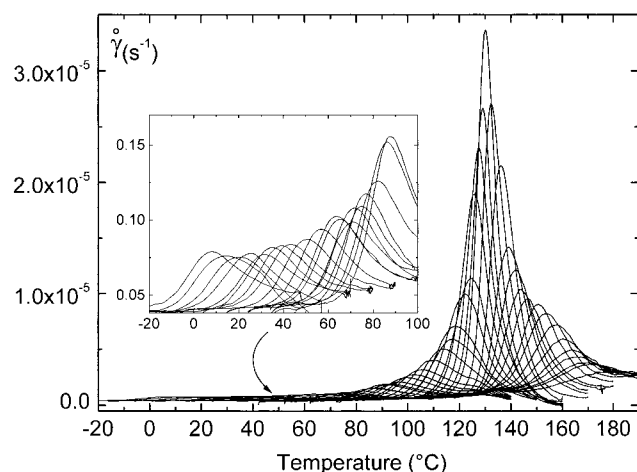


Figure 3. TSCR elementary spectra obtained in S-90 PMMA by the method of fractional loading. T_m varies by temperature step of 5 °C between 0 and 70 °C and 3 °C between 70 and 160 °C. The inset represents the experimental deconvolution of the onset of the α retardation mode.

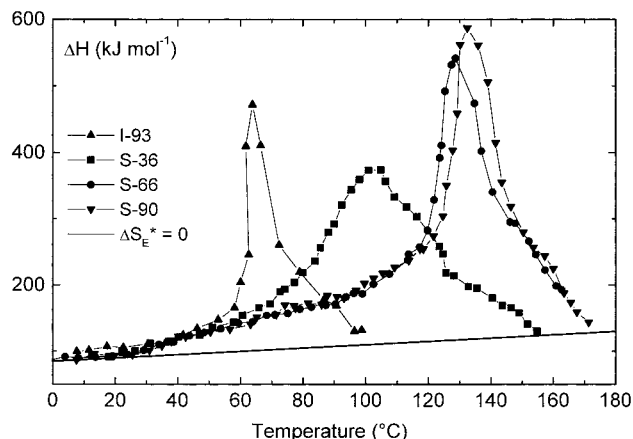


Figure 4. Activation enthalpy ΔH , as a function of temperature in I-93, S-36, S-66, and S-90 PMMA. The straight line corresponds to the zero entropy prediction ($\Delta S = 0$). The error bars are within the thickness of the symbols.

fractional loading (FL) procedure over the whole temperature scale of the TSCR global spectra. A series of FL-TSCR elementary spectra in PMMA S-90, resolved in the temperature range $-20 < T < 190$ °C, are shown in Figure 3. The "stress window" ($\Delta T_\sigma = 5$ °C) is shifted by steps of 5 °C in the temperature range 0–70 °C and by steps of 3 °C in the temperature range 70–160 °C to resolve α retardation process. FL-TSCR spectra are analyzed to determine the values of activation enthalpy and entropy between 0 and 180 °C.

The activation enthalpy ΔH obtained from eq 2 is plotted as the function of the maximum temperature T_m in Figure 4. T_m is the temperature of maximum intensity of each FL-TSCR elementary process (see Figure 3). To determine the activation entropy of α relaxation process, Starkweather^{12,13} has modified the Eyring's of activated states equation as follows:

$$\Delta H = RT \left[\ln \left(\frac{k_B}{2\pi\hbar} \right) + \ln \frac{T}{f} + 1 \right] + T\Delta S \quad (4)$$

where ΔS and ΔH are the activation entropy and enthalpy, respectively, and f is the relaxation frequency.

For simple relaxation, relatively few cooperative motions are required, and the activation entropy is then

close to zero.^{4,12,13,21–24} Complex relaxations, as α relaxation, have large positive activation entropies and involve cooperative motions of neighboring groups or molecules.^{4,12,13,21–24}

The solid line in Figure 4 is calculated using eq 4 where f is the equivalent frequency of TSCR, of about $(5 \pm 0.2) \times 10^{-3}$ Hz, and ΔS set equal zero. Several features can be observed for each sample: (i) The measured values of ΔH depart from the $\Delta S = 0$ prediction around 30 °C independent of tacticity. (ii) As expected, enthalpy rises drastically as temperature approaches T_g and exhibits a maximum at T_g . This behavior is generally observed in amorphous polymers investigated by thermally stimulated techniques.^{4,12,13,16,21–24} (iii) Above T_g , enthalpy drops rapidly. (iv) No negative values of ΔS are obtained in the investigated PMMA samples. (v) In the glass transition region, the values of ΔH in 36% syndio-triads sample are lower than those in I-93, S-66, and S90 samples. Note that S-36 exhibits the broadest "full width at half-maximum", ΔT_{TSCR} , of the enthalpy distribution. Evolution of ΔT_{TSCR} has been compared to the glass transition width, ΔT_{DSC} , determined according to Donth's method.²⁶ ΔT_{DSC} is the transformation interval between 16% and 84% of the total ΔC_p step in DSC thermograms. ΔT_{TSCR} and ΔT_{DSC} values are reported in Table 2. The tacticity dependences of ΔT_{TSCR} and ΔT_{DSC} are similar.

To understand the viscoelastic behavior of 36% syndio-triads PMMA sample, a 50/50 by weight blend of PMMA I-93 and PMMA S-66 has been investigated by TSCR and FL methods. The blend nearly displays the same tacticity as S-36 sample but with tacticity blocks distributed among both sample chains, and the average percent of iso-, hetero-, syndio-triads is 47, 35, and 28, respectively. Figure 5 shows the comparison of the TSCR spectra and ΔH temperature dependence between S-36 homopolymer and 50/50 I93/S66 PMMA blend. Except for a shift of 10 °C between the respective maxima, TSCR and FL behaviors of the blend and S-36 sample are similar. The temperature shift arises from the discrepancy in the isotactic and syndiotactic triads content. Temperature positions of the glass transition and α retardation mode of the PMMA blend are in agreement with the evolution of nonblended PMMA as a function of syndio-triad content (see Figure 2).

As shown in Figure 4, the distribution of relaxation times can be treated as a distribution in activation enthalpies. In S-66 and S-90 samples, three behaviors in the variation of ΔH with T_m can be observed. From 30 to 90 °C, ΔH increases slowly with T_m and departs from the $\Delta S = 0$ prediction. This increase is more rapid between 90 and 110 °C and become very drastic when T_m approaches T_g . In S-36 and I-93 samples, only the two last mentioned behaviors can be observed. The large temperature range where cooperativity takes place is a rather unique feature of PMMA. In S-90 PMMA, molecular motion cooperativity spreads over more than 100 °C.

The activation entropy for each FL-TSCR elementary peak is determined using eq 3 where T is the maximum temperature T_m . Activation enthalpy and entropy are increasing functions of T_m from 30 °C to the respective T_g of the various PMMA samples.

To check the presence of three various behaviors of activation enthalpy ΔH between 0 °C and T_g , the activation entropy ΔS has been reported versus ΔH (Figure 6). As shown in S-90 PMMA, a linear relation-

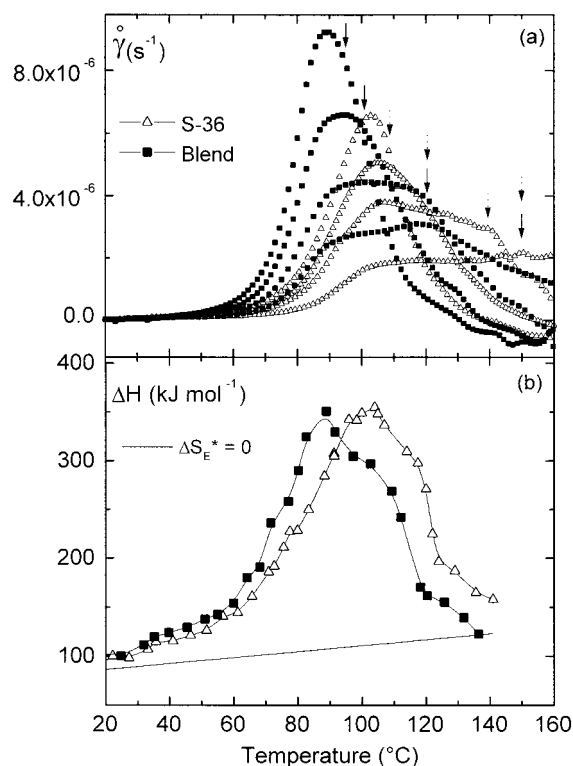


Figure 5. Complex TSCR spectra for S-36 and a 50/50 I-93 S-66 PMMA blend. The respective loading temperatures are symbolized by arrows (a). Temperature dependence of the activation enthalpy ΔH in S-36 and a 50/50 wt % I-93/S-66 PMMA blend (b). The error bars are within the thickness of the symbols.

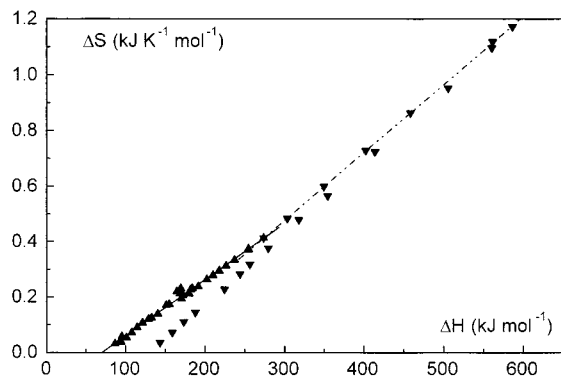


Figure 6. Compensation diagram for activation parameters in S-90 PMMA. The dash-dotted and solid linear curves represents the compensation laws (eq 5) for the α retardation mode and its onset (see inset of Figure 3), respectively. The error bars are within the thickness of the symbols.

ship exists between ΔS and ΔH for several FL-TSCR elementary processes. This relationship is well-known as the compensation rule^{8,10,16,22,24,26–35} and can be written as

$$\Delta S = \frac{\Delta H}{T} + S_0 \quad (5)$$

where S_0 is a constant. For all the samples only two linear behaviors (compensation rules) are observed. As expected in polymers investigated by thermally stimulated techniques,^{8,10,16,22,26–30,33–35} a well-defined linear relationship between ΔS and ΔH is observed for the TSCR α peak associated with the glass transition (defined as the temperature range where the drastic

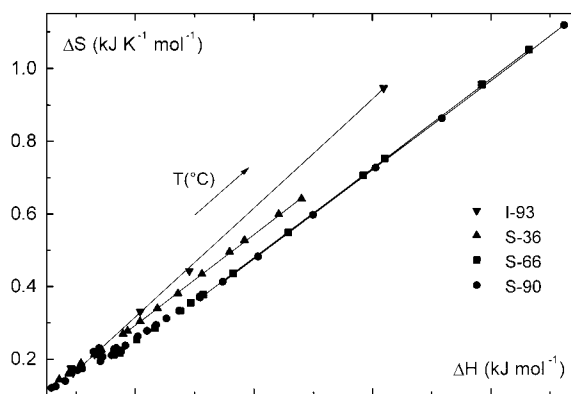


Figure 7. Compensation diagram for activation parameters of the α retardation mode in I-93, S-36, S-66, and S-90 PMMA. The solid linear curves represent the compensation laws (eq 5). The error bars are within the thickness of the symbols.

increase of enthalpy occurs), independent of the microstructure. The elementary processes isolated in the temperature range before the drastic increase of ΔH lead to a separate compensation law as well.

An interesting feature of the compensation diagram is the microstructure dependence of the compensation law in the glass transition region. From Figure 7, a comparison between the TSCR–FL fine structure of the various PMMA samples can be performed in the α retardation region. For a given ΔH value, taken between 250 and 350 kJ mol^{-1} , ΔS is similar in S-90 and S-66 samples but is higher in S-36 and I-93 samples.

Discussion

As previously observed by Sauer⁴ from thermally stimulated depolarization current (TSDC) and thermal sampling (TS) methods, the temperature T_α of the TSCR α peak in PMMA increases with syndiotactic triads content. The TSCR study covers a broader range of syndiotactic triads content than that of the TSDC⁴ investigation, particularly at low content. In this range, the S-36 PMMA displays, through the FL-TSCR peaks analysis, a viscoelastic response significantly different of the highly syndiotactic PMMA (Figure 4).

On the contrary of Sauer's TSDC results,⁴ the temperature at which a significantly departure from the $\Delta S = 0$ prediction occurs is independent of the tacticity and is about 30 $^{\circ}\text{C}$. Another discrepancy between TSCR and TSDC results is that the magnitude of activation energy E_a obtained from TS analysis at T_g is nearly independent of the tacticity and is about of 350 kJ mol^{-1} in average. The determined mechanical activation energy at T_g is greater than 350 kJ mol^{-1} and varies with syndiotactic triads content. T_g (or T_α) shifts toward high temperatures as syndio-triads percentage increases. This shift is discussed in the framework of inter- or intramolecular interactions, chain stiffness, and chain conformation. Isotactic PMMA is characterized by a symmetric stiff chain^{1,19,36} arising from a high ability to establish localized intramolecular interactions. We define "localized interactions" as interactions between consecutive ester groups belonging to the same chain. Syndiotactic PMMA chains are more coiled³⁶ than isotactic chains, with loops of 1.5–5 nm, and are accordingly less stiff.^{1,19,36} As a first consequence, isotactic chains are better packed than syndiotactic chains: the density is 1.21 and 1.18, respectively.² Considering the above parameters, the high-tempera-

ture position of the α retardation process and high values of activation enthalpies at T_g observed in syndiotactic PMMA are rather unexpected compared with those of the isotactic PMMA. Taking into account this remark and the fact that the cohesive energy density CED_R (proportional to the solubility parameter as $\delta^{1/2}$) increases from 9.28 to 9.55 as syndio-diads content increases³⁷ from 5 to 92%, the syndiotactic PMMA is characterized by strong intermolecular interactions. Their presence is responsible for the molecular mobility restriction so that T_g increases. Furthermore, they allow large cooperative persistence lengths which involve high ΔH at T_g . In I-93, the persistence length of cooperative motion is due to stiff well-packed chains and leads to cooperative domains smaller than in S-90 samples (see below and ref 23). The lack of strong intermolecular interactions in I-93 PMMA involves a lower T_g than in the S-90 sample.

The behavior of the compensation law with tacticity (see Figure 7) gives some information on the mobility released in the α retardation mode. No difference is noticeable between S-66 and S-90 samples listed as very low iso-triads content (1–2%) PMMA. On the other hand, for a fixed activation enthalpy the activation entropy raises as the iso-triads content increases from 2 to 93%. The observed difference between S-66 or S-36 and I-93 samples increases with increasing activation enthalpy. It is only for the processes in the α region that differences between each sample become obvious. The degree of cooperative motion involved with the α retardation process can be estimated from the activation entropy ΔS . As temperature approaches T_g , the α retardation mode in I-93 PMMA involves clearly more cooperative motion than the same process found in the various syndiotactic samples. The activation entropy behavior reflects the effect of the iso-triads content on the degree of cooperativity of the molecular motions responsible of α retardation process.

The FL-TSCR behavior of PMMA S-36 is more questioning, because it is the worst packed polymer² and its chain stiffness is quite high compared with that of isotactic or syndiotactic PMMA.^{38,39} Nevertheless the glass transition temperature T_g is relatively high, about 105 °C. The full width at half-maximum of the ΔH_f peak and glass transition broadness ΔT_{DSC} are large compared with those of other samples. According to Donth,²⁵ ΔT_{DSC} is inversely proportional to the size of domains where cooperativity takes place at T_g . This is in agreement with the weak value of ΔH obtained in S-36 sample at T_g . Because of the large width of the α relaxation in the enthalpic diagram, the cooperative domains are many but smaller than in pure tactic species. Mechanical loss curves for blend or S-36 PMMA display a very broad α relaxation peak in the temperature domain⁴⁰ characteristic of glass heterogeneity. Stereoblock PMMA or isotactic/syndiotactic blends are assumed to form a stereocomplex⁴⁰ in a peculiar solvent or under specific temperature conditions. The same TSCR spectra and ΔH temperature dependence are observed for the blend and S-36 samples (see Figure 5). The relative high T_g of S-36 is not fully understood: either stereocomplex-like interactions are formed, or the syndio-triads amount is important enough to establish interchain interactions. Partially miscibility of iso- and syndiotactic sequences would explain the important ΔT_{DSC} value at T_g .

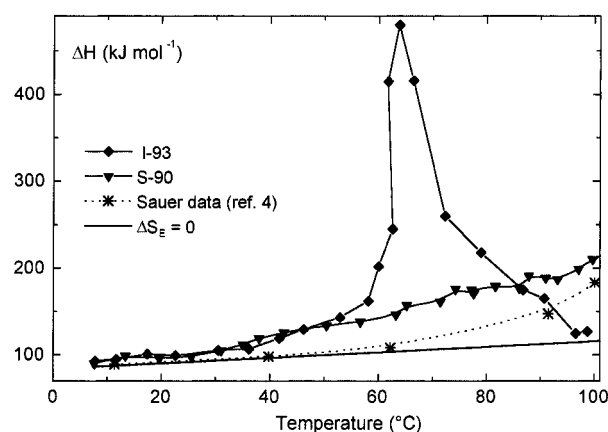


Figure 8. Activation enthalpy, ΔH , as a function of temperature in I-93, S-90, and ref 4 PMMA. The straight line corresponds to the zero entropy prediction ($\Delta S = 0$).

The other important feature of ΔH – T curves is the departure from the $\Delta S = 0$ prediction around 30 °C, independent of tacticity of samples. Cooperative motions, in the Starkweather framework, spread over 130 °C for a rich syndiotactic PMMA. We have reported in Figure 8 the values of the activation enthalpy at various temperatures obtained by Sauer⁴ using the TSDC-TS method in a syndiotactic PMMA with an iso-triads content lower than 0.1%. The activation enthalpies' departure from the $\Delta S = 0$ prediction is observed around 70–80 °C in Sauer's samples (see Figure 8). Unlike rich isotactic PMMA, I-93, or an isotactic PMMA (see refs 2 and 4), the ΔH maximum is in the 50–60 °C temperature range. Because our syndiotactic PMMA samples involve an amount of iso-triad sequences different from the samples studied by Sauer, the onset of the α relaxation arises from the presence of iso-triads along the chain. Sauer suggested that isotactic-rich sequence pockets (at least 2 nm for glass-transition-like motion) are responsible for the onset of cooperativity in this temperature range. This would be supported by the fact that PMMA of different tacticities blend is borderline miscible as indicated by the very broad glass transition domain (see Figure 5). Moreover, pure isotactic and syndiotactic PMMA are certainly immiscible. However, even ΔH values, obtained in the S-90 sample, depart from the $\Delta S = 0$ prediction at 30 °C with the same magnitude as the other PMMA samples. The existence of rich iso-triads pockets in the S-90 sample is therefore doubtful because its iso-triads content is only 1%.

Schmidt-Rohr's NMR results⁴¹ show that about 50% of the ester groups undergo, at 60 °C, π flips coupled with main chain conformational changes. Tordjeman et al.⁴² performed DMA measurements on MMA–maleimide copolymers. The stiff maleimide units were introduced to hinder large-scale conformational motions. The amplitude of the β cooperative process that is associated with the high-temperature ester motion coupled to the main chain motions decreases as the maleimide content increases. In the same way, we suggest that the introduction of iso-triads along a chain enhances the mobility in this temperature range and favors ester flips coupled to the main chain motions. The study of PMMA samples with short persistence length iso-triads sequences, well distributed along the chain, will be necessary to confirm this assumption.

As indicated previously, before the sharp ΔH increase at T_α , there is a monotonic change in the ΔH temper-

ature dependence. This evolution is notified by a well-separated compensation phenomenon (see Figure 6) in the 100–250 kJ mol⁻¹ enthalpy range. The FL–TSCR elementary processes, involved in this phenomenon, are characterized by ΔH and ΔS values clearly lower than those obtained in the α relaxation. Such a behavior has been described elsewhere.^{29,43,44} These FL–TSCR elementary processes can be attributed to similar motions of chain segments shorter than those responsible for the main α mode and interpreted as a precursor of the α retardation process.²⁹

Conclusion

The study of PMMA of various tacticity by the FL–TSCR method reveals the α retardation mode broadness. Indeed, iso-triad sequences allow cooperative motions as soon as 30 °C, far below the glass transition but above the secondary β relaxation. Definite nature and iso-triads contribution to this cooperative onset must be however confirmed by forthcoming studies. Above this onset, first ΔH monotonically increases, then sharply increases when temperature approaches T_g , and passes through a maximum at T_g . The temperature range, involving cooperative motions, extends over more than 100 °C. Both the width and the maximum value of the ΔH – T plot around T_g are highly tacticity dependent. The observed various behaviors are explained in terms of molecular interactions and suggest the existence of high intermolecular interactions in syndiotactic PMMA contrary to the isotactic PMMA. This characterization also reveals the glass heterogeneity on S-36 and the isotactic/syndiotactic PMMA blend.

References and Notes

- Jasse, B.; Oultache, A. K.; Mounach, H.; Halary, J. L.; Monnerie, L. *J. Polym. Sci., Polym. Phys. Ed.* **1996**, *34*, 2007.
- Gourari, A.; Bendaoud, M.; Lacabanne, C.; Boyer, R. F. *J. Polym. Sci., Polym. Phys. Ed.* **1989**, *23*, 889.
- Biros, J.; Larina, T.; Trekoval, J.; Pouchly, J. *Colloid Polym. Sci.* **1982**, *260*, 27.
- Sauer, B. B.; Kim, Y. H. *Macromolecules* **1997**, *30*, 3323.
- Lacabanne, C.; Chatain, D.; Monpagens, J. C. *J. Macromol. Sci., Phys.* **1977**, *B134*, 537.
- Monpagens, J. C.; Lacabanne, C.; Chatain, D.; Hiltner, A.; Baer, E. *J. Macromol. Sci., Phys.* **1978**, *B15* (4), 503.
- Lacabanne, C.; Chatain, D.; Monpagens, J. C.; Berticat, P. *J. Appl. Phys.* **1979**, *50*, 2723.
- Demont, P.; Chatain, D.; Lacabanne, C.; Ronarc'h, D.; Moura, J. L. *Polym. Eng. Sci.* **1984**, *24*, 127.
- Diffalah, M.; Demont, P.; Lacabanne, C. *Thermochim. Acta* **1993**, *226*, 33.
- Boye, J.; Demont, P.; Lacabanne, C. *J. Polym. Sci., Polym. Phys. Ed.* **1994**, *32*, 1359.
- Dufresne, A.; Etienne, S.; Perez, J.; Demont, P.; Diffalah, M.; Lacabanne, C.; Martinez, J. J. *Polymer* **1996**, *37*, 2359.
- Starkweather, H. W. *Macromolecules* **1981**, *14*, 1277.
- Starkweather, H. W. *Polymer* **1991**, *32*, 2443.
- Ute, K.; Miyatake, N.; Hatada, K. *Polymer* **1995**, *36*, 1415.
- Gillham, J. K. *Polym. Eng. Sci.* **1979**, *19*, 749.
- Doulut, S. Ph D. Thesis, Université de Toulouse, France, 1998.
- Bucci, C.; Fieschi, R.; Guidi, G. *Phys. Rev.* **1966**, *146*, 816.
- Glasstone, S.; Laidler, K. J.; Eyring, H. *The Theory of Rate Processes*; McGraw-Hill: New York, 1942.
- Fuchs, K.; Friedrich, C.; Weese, J. *Macromolecules* **1993**, *29*, 7134.
- Yasuda, H.; Yamamoto, L.; Yamashita, M.; Yokota, K.; Nakomura, A.; Miyake, S.; Kai, Y.; Kaneshisa, N. *Macromolecules* **1993**, *26*, 7134.
- Demont, P.; Diffalah, M.; Martinez-Vega, J. J.; Lacabanne, C. *J. Non-Cryst. Solids* **1994**, *172–174*, 978.
- Sauer, B. B.; Avakian, P. *Polymer* **1992**, *33*, 5128.
- Nogales, A.; Sauer, B. B. *J. Polym. Sci., Polym. Phys. Ed.* **1998**, *36*, 913.
- Doulut, S.; Demont, P.; Lacabanne, C. *J. Therm. Anal.* **1998**, *51*, 805.
- Donth, E. *J. Polym. Sci., Polym. Phys. Ed.* **1986**, *34*, 2881.
- Zielinski, M.; Swiderski, T.; Kryszewski, M. *Polymer* **1978**, *19*, 883.
- McCrum, N. G.; Pizzoli, M.; Chai, C. K.; Treurnicht, I.; Hutchinson, J. M. *Polymer* **1982**, *23*, 473.
- Ronarc'h, D.; Audren, P.; Moura, J. P. *J. Appl. Phys.* **1985**, *58*, 474.
- Colmenero, J.; Alegria, A.; Alberdi, J. M.; Del Val, J. J.; Ucar, G. *Phys. Rev. B* **1987**, *35*, 1987.
- Del Val, J. J.; Colmenero, J. *Makromol. Chem.* **1989**, *190*, 893.
- Crine, J. P. *J. Phys. D: Appl. Phys.* **1990**, *23*, 1315.
- Perez, J.; Cavaille, J. Y. *J. Phys. III* **1995**, *5*, 791.
- Tesseydre, G.; Demont, P.; Lacabanne, C. *J. Appl. Phys.* **1996**, *79*, 9258.
- Moura Ramos, J. J.; Mano, J. F.; Sauer, B. B. *Polymer* **1997**, *38*, 1997.
- Doulut, S.; Bacharan, C.; Demont, P.; Bernes, A.; Lacabanne, C. *J. Non-Cryst. Solids* **1998**, *235–237*, 645.
- Cowie, J. M. G. *Polymer* **1969**, *10*, 708.
- Appel, U. M.; Hentschke, R.; Helfrich, J. *Macromolecules* **1995**, *28*, 1778.
- Vacatello, M.; Flory, P. J. *Macromolecules* **1986**, *19*, 405.
- Jenkins, R.; Porter, R. S. *Adv. Polym. Sci.* **1980**, *36*, 1.
- Allen, P. E. M.; Host, D. M.; Truong, V. T.; Williams, D. R. G. *Eur. Polym. J.* **1985**, *21*, 603.
- Schmidt-Rohr, K.; Kulik, A. S.; Beckham, H. W.; Ohlmacher, A.; Pawelzik, U.; Boeffel, C.; Spiess, H. W. *Macromolecules* **1994**, *27*, 4733.
- Tordjeman, P.; Teze, L.; Halary, J. L.; Monnerie, L. *Polym. Eng. Sci.* **1997**, *3*, in press.
- Colmenero, J.; Alegria, A.; del Val, J. J.; Alberdi, J. M. *Makromol. Chem. Symp.* **1988**, *20–21*, 397.
- Del Val, J. J.; Colmenero, J.; Mijongos, C.; Martinez, G.; Millán, J. L. *Makromol. Chem.* **1989**, *190*, 893.

MA990247K